Biochemistry and Biophysics Reports 1 (2015) 22–32

Contents lists available at ScienceDirect

Biochemistry and Biophysics Reports

journal homepage: www.elsevier.com/locate/bbrep

Structural and functional comparison of hexahistidine tagged and untagged forms of small multidrug resistance protein, EmrE

S. Junaid S. Qazi, Raymond Chew, Denice C. Bay, Raymond J. Turner *

Department of Biological Sciences, University of Calgary, Calgary, Alberta, Canada T2N 1N4

ARTICLE INFO

Article history:
Received 22 February 2015
Received in revised form
13 March 2015
Accepted 18 March 2015
Available online 26 March 2015

Keywords:
Small multidrug resistance (SMR) protein
EmrE
Integral membrane protein folding
Quaternary ammonium compounds (QAC)
Quaternary cation compounds (QCC)
Hexahistidine (His_6) tag

ABSTRACT

EmrE is a member of the small multidrug resistance (SMR) protein family in *Escherichia coli*. EmrE confers resistance to a wide variety of quaternary cation compounds (QCCs) as an efflux transporter driven by proton motive force. The purification yield of most membrane proteins are challenging because of difficulties in over expressing, isolating and solubilizing them and the addition of an affinity tag often improves purification. The purpose of this study is to compare the structure and function of hexahistidinyl (His_6) tagged (T-EmrE) and untagged (UT-EmrE) versions of EmrE. *In vivo* QCC resistance assays determined that T-EmrE demonstrated reduced resistance as compared to UT-EmrE. We isolated EmrE using the two different purification methods, an organic solvent extraction method used to isolate UT-EmrE and nickel affinity chromatography of T-EmrE. All proteins were solubilized in the same buffered n-dodecyl-β-D-maltopyranoside (DDM) detergent and their conformations were examined in the presence/absence of different QCCs. *In vitro* analysis of protein multimerization using SDS-Tricine PAGE and dynamic light scattering analysis revealed that both proteins predominated as monomers, but the formation of dimers was more constant and uniform in T-EmrE compared to UT-EmrE. The aromatic residue conformations of both proteins indicate that T-EmrE form is more aqueous exposed than UT-EmrE, but UT-EmrE appeared to have a more dynamic environment surrounding its aromatic residues. Using fluorescence to obtain QCC ligand-binding curves indicated that the two forms had differences in dissociation constants (K_d) and maximum specific one-site binding (B_{max}) values for particular QCCs. *In vitro* analyses of both proteins demonstrated subtle but significant differences in multimerization and QCC binding. *In vivo* analysis indicates differences caused by the addition of the tag, we also observed differences *in vitro* that could be a result of the tag and/or the different purification methods.

© 2015 The Authors. Published by Elsevier B.V. This is an open access article under the CC BY-NC-ND license (http://creativecommons.org/licenses/by-nc-nd/4.0/).

1. Introduction

Escherichia coli multidrug resistance transporter E (EmrE) is an integral membrane protein that is 110 amino acids in length and is considered to be the archetypical member of the small multidrug resistance (SMR) family transporters [1,2]. EmrE is one of many transporters responsible for antiseptic drug resistance in bacteria by the efflux of toxic quaternary cationic compounds (QCCs) [3,4]. EmrE is composed of 4 transmembrane spanning alpha helices connected by short loops (as reviewed by Bay et al. [2]). EmrE has been shown to exist as a monomer, dimer, trimer, tetramer or even higher ordered multimers/complexes but the minimal functional unit is considered to be a dimer [5–9].

Due to the high proportion of hydrophobic residues in EmrE, it can partition into and be purified from organic solvents. Initial studies of EmrE involved an organic solvent mixture of 1:1 chloroform:methanol to extract and isolate EmrE from *E. coli* membranes [3]. Following organic extraction, lipophilic chromatography techniques were used for the purification of EmrE [10]. Another purification method involved the fusion of a hexahistidine (His_6) tag onto the C-terminus to purify EmrE using immobilized Ni^{2+} affinity chromatography techniques [11]. This His_6 modification is commonly used in most structural analyses of EmrE protein (as reviewed by Bay et al. [2]). However, the influence of the His_6 tag on structure and activity can depend on the position of its attachment to the protein [12]. Almost all tagged EmrE protein *in vitro* studies have involved a fusion tag that includes a *myc* epitope linker attached to the His_6 sequence on the C-terminus (EmrE-*myc*-His_6), which was shown to improve protein expression and functional activity (as described by Muh and Schuldiner [5]). Since its publication, this EmrE-*myc*-His_6 tagged version has been used to study the biochemistry and biophysical conformation of EmrE protein over the past decade.

* Correspondence to: University of Calgary, Rm BI487, Biological Sciences Bldg., 2500 University Dr. NW, Calgary, Alberta, Canada T2N 1N4. Tel.: +1 403 220 4308; fax: +1 403 289 9311.

E-mail addresses: sjsqazi@ucalgary.ca (S.J.S. Qazi), raychew18@gmail.com (R. Chew), dbay@ucalgary.ca (D.C. Bay), turnerr@ucalgary.ca (R.J. Turner).

http://dx.doi.org/10.1016/j.bbrep.2015.03.007
2405-5808/© 2015 The Authors. Published by Elsevier B.V. This is an open access article under the CC BY-NC-ND license (http://creativecommons.org/licenses/by-nc-nd/4.0/).

The primary sequences of previously characterized untagged (UT-) and tagged (T-) EmrE are shown in Fig. 1. T-EmrE has been extensively studied structurally and biochemically and serves as the model SMR family protein [13]. High-resolution 3D analysis using cryo-electron microscopy and X-ray diffraction crystallography has reported the conformational state of asymmetric dimer for T-EmrE [8,14,15]. NMR studies of T-EmrE have also shown that it forms a functional dimer, where both Glu14 ligand binding active site residues from each monomer were located in structurally inequivalent environments [16]. In addition to Glu14, previous studies of T-EmrE have identified the involvement of aromatic residues in ligand binding. Trp63 was demonstrated to be located close to the QCC binding pocket and deemed important for ligand binding as a mutation at this position abolished substrate binding [4,17]. Two other tryptophans located within transmembrane segments 2 and 3 and the fourth tryptophan can be found in loop 2 of both proteins, however both UT- and T-EmrE also have 5 and 6 tyrosines respectively. Although the majority of published work on EmrE has focused on T-EmrE and to a lesser extent UT-EmrE (as reviewed by Bay et al. [2]), a direct comparison between both forms of the protein have never performed. Confounding and sometimes conflicting EmrE ligand binding data [5,7,14,18–20] provided in Table 1 that highlights the differences in ligand binding constants of T-EmrE and UT-EmrE.

The goal of this study was to compare UT-EmrE and T-EmrE preparations analyzed under the same detergent conditions using the same biochemical and biophysical techniques to identify the similarities and differences between their structures and functions. The aim of this study was to compare EmrE proteins isolated using their respective purification methods as reported for UT-EmrE [9,21] and for T-EmrE [22] in side by side in the same *in vivo* and *in vitro* experiments. The outcome will ideally resolve some of the differences that have been reported between different groups. A comparison of *in vivo* QCC resistance for the two forms revealed different resistance profiles. Upon purification, UT-EmrE and T-EmrE were reconstituted into the same buffer conditions containing 0.08% w/v n-dodecyl-β-D-maltopyranoside (DDM). Four different but commonly examined QCCs were selected for testing UT-EmrE and T-EmrE. Both forms of the protein were evaluated using Sodium dodecyl sulfate (SDS)-Tricine polyacrylamide gel electrophoresis (PAGE), dynamic light scattering (DLS) and fluorescence spectroscopy. SDS-Tricine PAGE and DLS techniques were used to compare the size and multimeric state of both proteins. Intrinsic Trp fluorescence analysis was used to determine changes in the environment of tryptophans and tyrosines, as they provide insight into chemistry of their immediate surroundings and excited state and relaxation dynamics of the protein. Changes in fluorescence emission maximum and intensity by both versions of the protein were also compared to determine any differences in Trp quenching caused by QCC binding in the protein. Using the same membrane mimetic detergent solubilization conditions, the *in vitro* comparison of UT-EmrE and T-EmrE in 0.08% w/v DDM reflected subtle differences in how each protein interacted with itself as a multimer and with each of the four QCCs tested. The aromatic residue conformations of both proteins indicate that T-EmrE form is more open to aqueous than UT-EmrE, but UT-EmrE has multiple environments surrounding its aromatic residues suggesting more dynamics. Fluorescent ligand binding experiments performed with UT-EmrE and T-EmrE also determined that the tag may provide a conformation that restricts the binding of certain QCC. This study highlights the subtle variations in function and conformation of EmrE.

2. Material and methods

2.1. Materials

The chemicals used in this study were purchased from either Sigma Aldrich (St. Louis, MO, USA) or EMD Chemicals (Darmstadt, Germany). Electrophoresis equipment and electrophoretic chemicals were obtained from BioRad (Hercules, CA, USA). The DDM detergent, used for protein solubilization and spectroscopy was purchased from Affymetrix-Anatrace (Santa Clara, CA, USA).

2.2. In vivo E. coli QCCs resistance assays of UT-EmrE and T-EmrE

Both UT-EmrE and T-EmrE were cloned in the expression vector pMS119EH resulting in the plasmids pEmr11 and pEmrEmLVH6, respectively. Both genes were expressed with this vector using the isopropyl β-D-1-thiogalactopyranoside (IPTG) inducible *tac* promoter and permitted the expression of both constructs under identical conditions. Expression of either EmrE construct was not induced by IPTG nor was it added to the growth media during any resistance assays. Previous studies confirmed that the expression 'leakiness' from the pMS119EH *Ptac* was appropriate for biological assays of EmrE [23,24].

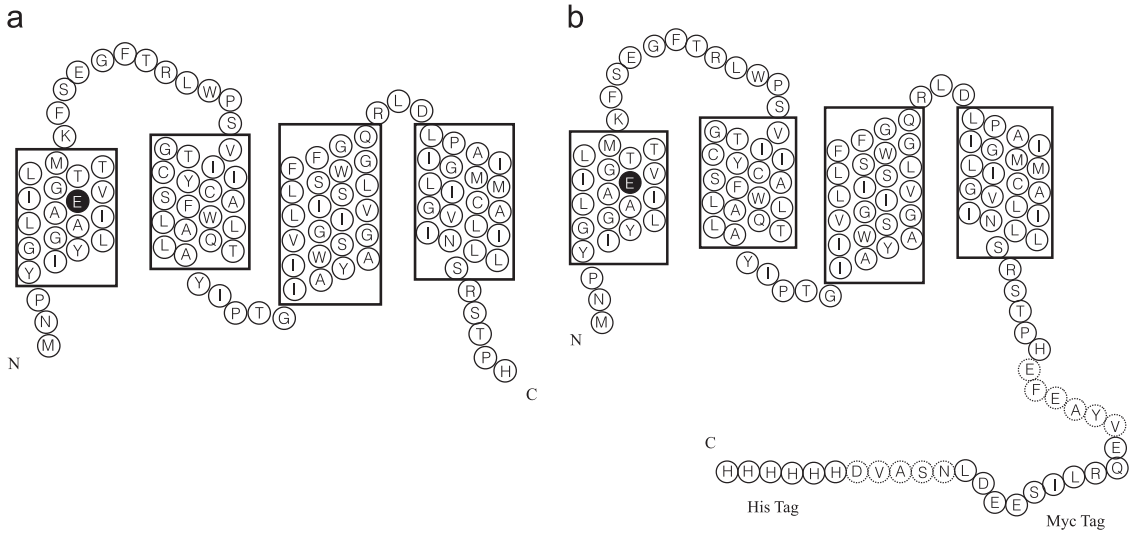

Fig. 1. (a) UT-EmrE and (b) T-EmrE amino acid sequences that were examined in this study. Boxes indicated predicted transmembrane regions for each protein.

Table 1
Binding affinities of QCCs to tagged and untagged EmrE evaluated under different conditions from previous studies.

Assaying condition	Experiment	Ligand	K_d (μM)	Reference
T-EmrE				
0.08% w/v DDM	Equilibrium dialysis	[^{3}H] TPP	0.01 ± 0.003	[5]
0.8% w/v DDM	Saturation binding assay	[^{3}H] TPP	0.0028 ± 0.001	[18]
0.1% w/v DDM	Saturation binding assay	[^{3}H] TPP	0.0026 ± 0.0004	[14]
0.5% w/v DDM (delipidated EmrE)	Saturation binding assay	[^{3}H] TPP	2.5 ± 0.5	[19]
0.5% w/v DDM (non-delipidated EmrE)			10 ± 2	
UT-EmrE				
Small unilamellar vesicle (SUV)	Isothermal Titration Calorimetry (ITC)	EB	5.5 ± 2.1	[20]
		MV	38.2 ± 8.7	
		Pro	10.7 ± 2.8	
8% w/v SDS		EB	5.2 ± 1.4	
		MV	5.4 ± 1.2	
		Pro	4.5 ± 0.8	
		TPP	4.8 ± 0.8	
2% w/v DDM		EB	6.3 ± 1.0	
		MV	46.2 ± 10.5	
		Pro	5.2 ± 0.9	
		TPP	25.5 ± 6.2	
2% w/v DDM	Fluorescence	EB	6.8 ± 0.5	[7]
		MV	43.6 ± 3.8	
		TPP	23.6 ± 7.1	
		CTP	6.6 ± 2.2	

E. coli cells were cultured on a LB streak plate containing 0.1 mg/mL ampicillin. Colonies were picked and mixed into a 0.9% saline solution until the turbidity matched a 1.0 Mcfarland standard. The solution was then used to inoculate 96-well plates containing LB growth media. A dilution series of QCCs, ethidium bromide (EB), methyl viologen (MV), cetylpyridinium chloride (CTP) and tetraphenyl phosphonium (TPP) were prepared. QCC serial dilutions started at a concentration of 5 mg/mL in a well up to 9.8 μg/mL, using a 1/2 dilution step in each preceding well. A well without QCC was also included as a growth control. Spot plates containing LB and 0.1 mg/mL ampicillin were used to verify the cell numbers estimated by the 1.0 Mcfarland standard. Spot plates were incubated for 12–16 h at 37 °C before counting colonies. Growth plates were incubated at 37 °C and removed from the incubator every hour for 11 h to record the optical densities (OD) of each well at 550 nm ($OD_{550\ nm}$) using a microtiter plate reader. Plates were incubated at 37 °C for an additional 26 h after inoculation and its $OD_{550\ nm}$ was recorded. A series of "blank" wells containing only growth media or growth media and QCC was included on the plates for the background subtraction from the sample. Data were collected and averaged over 3 biological replicates. The result of this approach is a viability kill curve titration.

2.3. Expression and purification of UT- and T-EmrE proteins

A brief description on the expression and purification procedure for both UT- and T-EmrE is provided in the following sections.

2.3.1. UT-EmrE protein accumulation, organic extraction and reverse phase HPLC purification

The expression and purification of UT-EmrE were performed using the procedure described previously [9]. Briefly, LE392Δunc cells containing the pEmrE11 plasmid were cultured in 1 L batches of terrific broth (TB) (12 g/L tryptone, 24 g/L yeast extract, 0.4% v/v glycerol). Each 1 L culture batch was inoculated with 10 mL of overnight culture in Lysogeny broth (LB) (10 g/L tryptone, 5 g/L yeast extract, 5 g/L NaCl). All cultures contained 0.1 mg/mL ampicillin to maintain the plasmids during cell growth. The cultures were incubated at 37 °C and growth were monitored using $OD_{600\ nm}$ measurements. Once the $OD_{600\ nm}$ of the cultures reached between 0.5 and 0.7 (approximately 3 h), IPTG was added to the final concentration of 0.1 mM. Cultures were incubated at 37 °C in a shaking incubator for another 3 h. Cells were harvested and washed in SMR-A buffer (50 mM MOPS, pH 7.5, 5 mM EDTA, 1 mM DTT, 8% w/v glycerol) by stirring. The cells were re-pelleted by centrifugation at 4000*g* for 10 min at 4 °C and the supernatant was discarded. Cell yield was ~4 g per 1 L batch of culture that was re-suspended in 1–2 mL of SMR-A buffer per gram of the wet cell weight and stored frozen at −80 °C. Frozen cell suspensions were thawed on ice and a serine protease inhibitor phenylmethyl sulphonylfluoride (PMSF) was added to a final concentration of 0.1 mM and passed through the French Press twice at 10,000 psi to lyse the cells at 4 °C. Unbroken cells were separated by centrifugation at 2000*g* for 10 min and the supernatant was collected and subjected to further centrifugation at 120,000*g* for 90 min at 4 °C to collect the membrane pellet. The membrane pellet was re-suspended by homogenization in SMR-A buffer and stored at −80 °C.

The stored membrane sample was thawed and UT-EmrE protein was extracted from the membrane by organic extraction in 3:1 choroform:methanol solvent and concentrated using a rotovap apparatus as described by Schwaiger et al. [10] and Butler et al. [19]. The concentrated membrane organic extraction was separated by reverse-phase fast pressure liquid chromatography (FPLC) on AKTA™ Unicorn instrument (GE Lifesciences) using SR10/25 column with LH20 sephadex resin in 1:1 chloroform: methanol solvent. UT-EmrE protein eluted within the first peak as monitored by UV absorption at 280 nm ($A_{280\ nm}$) and SDS-Tricine PAGE analysis of fractions. UT-EmrE protein fractions were pooled together and dried under N_2 gas before storing at −20 °C. Proteins in each dried tube were collected from 3 L of cultures.

2.3.2. UT-EmrE protein solubilization in buffer containing DDM detergent

Dried UT-EmrE proteins were solubilized in a buffer containing DDM (20 mM Tris–HCl, pH 7.5, 150 mM NaCl, 0.08% w/v DDM). 1 mL of the buffer was added to each tube of dried UT-EmrE proteins. The suspension was vortexed for 2 h at room temperature and then centrifuged at 14,000*g* for 10 min to remove insoluble material. The pellet was discarded and the protein

concentration of the supernatant was determined by a modified Lowry assay [25]. The sample was then stored at −80 °C in small aliquots for further analysis.

2.3.3. T-EmrE protein accumulation and purification

The T-EmrE, containing EmrE with a myc epitope His_6 tag as described by Miroux and Walker [26] was cloned in the pTZ-19R plasmid (pTZEmrEmH6). Plasmid encoded T-EmrE was expressed in the *E. coli* strain C43(DE3) (F^- *ompT hsdSB* (rB– mB–) *gal dcm* (DE3)). C43(DE3) cells containing the pTZEmrEmH6 plasmid were cultured in 1 L batches of LB broth. Inoculation and initial growth conditions were identical to UT-EmrE expression until each culture reached an $OD_{600\ nm}$ between 0.5 and 0.7 (approximately 4–5 h) and were induced with 0.3 mM IPTG. Cultures were incubated for an additional 3 h at 37 °C and then cells were harvested by centrifugation using the same procedure as described for UT-EmrE cultures. Harvested cells were stored in re-suspension buffer (20 mM Tris–HCl, pH 8.2, 50 mM NaCl) and frozen at −80 °C. The cell yield from this experiment was an average of 3.3 g per 1 L batch of the culture.

T-EmrE was isolated in a similar manner to what was reported by Miller et al. [22]. Frozen cells were thawed and lysed using a French Press exactly as described for the UT-EmrE preparation and membranes were isolated by the same UT-EmrE ultracentrifugation procedure. The T-EmrE containing membrane pellet obtained from the 6 L culture was re-suspended in 25 mL of a membrane solubilization buffer (40 mM Tris–HCl, pH 8.2, 100 mM NaCl, 4% (w/v) DDM, 10 mM 2-mercaptoethanol). Re-suspended T-EmrE containing membrane fractions were placed in 50 mL falcon tubes for overnight on a gently rocking incubator at 4 °C to fully solubilize all membrane proteins. The membrane protein dispersion was than ready for Ni^{2+}-affinity resin chromatography.

2.3.4. T-EmrE-immobilized nickel affinity chromatography

The membrane protein re-suspension from Section 2.3.3 was diluted 1:1 with distilled H_2O and centrifuged at 60,000*g* to pellet non-solubilized material. NaCl to the final concentrations of 350 mM and imidazole to 15 mM were added in the membrane suspension after centrifugation. This sample was loaded into a 1 mL HisTrap FF immobilized nickel column (GE healthcare, Canada) using an AKTA purifier (GE healthcare) system for protein isolation. After loading, the isolation conditions used to obtain T-EmrE involved an initial washing step with 20 column volumes (CV) of wash buffer (20 mM Tris–HCl, pH 8.3, 400 mM NaCl, 65 mM imidazole, 0.1% w/v DDM, 5 mM 2-mercaptoethanol) to remove non-specific proteins. The final step involved elution of the protein from the resin with 10 CV of elution buffer (20 mM Tris–HCl, pH 8.3, 25 mM NaCl, 200 mM imidazole, 0.1 % w/v DDM, 5 mM 2-mercaptoethanol). A single protein elution peak was observed by monitoring the absorbance of the elutions at 280 nm and the corresponding elution fractions were collected and desalted as described in Section 2.3.5.

2.3.5. T-EmrE HiTrap desalting chromatography

Eluted T-EmrE samples after Ni^{2+}-affinity chromatography were pooled together and 2 mL aliquots of the pooled sample were injected into a 5 mL HiTrap desalting column (GE healthcare, Canada) to remove the imidazole. The column was equilibrated with DDM buffer (20 mM Tris–HCl, pH 7.5, 150 mM NaCl, 0.08% w/v DDM) and the sample was exchanged into this buffer. 0.08% w/v DDM in this buffer corresponded to 1.6 mM DDM, which is well above of its critical micelle concentration (CMC) of 0.12–0.17 mM in the buffered solution. All of the eluted fractions were analyzed by SDS-Tricine (12%T) PAGE to confirm the presence and purity of T-EmrE. The presence of T-EmrE was also confirmed by Western blotting the gels onto nitrocellulose and immunoblotting with a conjugated anti-His_6 Horseradish peroxidase antibody (Life technologies, Canada). Desalted T-EmrE samples were pooled together and stored at −80 °C until they were thawed for further experiments.

2.4. UT-EmrE and T-EmrE protein concentration determination

The concentration of both purified proteins were determined using a modified Lowry Assay [25] containing SDS to assist in solubilizing membrane proteins. Serial dilutions of bovine serum albumin (BSA) were used as a protein standard. The stock concentration of reconstituted UT-EmrE in DDM and desalted T-EmrE in DDM buffer was determined to be 15 μM and 11 μM respectively.

2.5. SDS-Tricine PAGE analysis of UT-EmrE and T-EmrE proteins

DDM solubilized UT-EmrE and T-EmrE were evaluated using SDS-Tricine (12%T) PAGE to identify its multimeric forms according to its molecular weight (MW). During gel casting, a final concentration of 0.5% (v/v) trichloroethanol (TCE) was added to the gels to visualize tryptophan residues within each protein sample. TCE visualization was performed using UV irradiation at 302 nm according to the method described by Ladner et al. [27]. This in-gel TCE staining technique increased EmrE protein visibility by 62% in comparison to conventional Coomassie staining [28]. UT-EmrE and T-EmrE samples separated by SDS-Tricine PAGE were prepared in incubation buffer (12% w/v SDS, 30% V/V glycerol, 0.05% CBB, 150 mM Tris–HCl pH 7.0, 100 mM DTT) from frozen stock samples of both proteins. Both samples were mixed by stirring and incubated at room temperature for 30 min. 20 μL of each sample was loaded into each gel lane. The protein samples were allowed to run for 5 h between 40 and 90 V to migrate the proteins according to their molecular weight. BioRad low range molecular weight (LMW) standards were used to compare the EmrE distribution on the gel. The loaded LMW standard had 1 μg of each protein whereas both UT-EmrE and T-EmrE samples had 1.4 μg of each protein. The gel was fixed prior to imaging with Kodak 1D software (V 3.6.5) using a gel fixing solution (50% v/v methanol, 10% v/v acetic acid) for 15–20 min.

2.6. Dynamic light scattering

Measurements of dynamic Light Scattering (DLS) from dispersed UT-EmrE and T-EmrE proteins with and without QCC were made in Nanoscience lab NANS at the University of Calgary. Data were collected at Zetasizer Nano-ZS by Malvern instruments with a He–Ne laser set to a wavelength of 633 nm and a power setting of 4.0 mW as a light source. Software was set to collect three runs for each sample. Size distributions on UT- and T-EmrE proteins in terms of intensity averages were obtained using Malvern instruments software V 7.02. The instrument uses Non-Invasive Back-scatter optics (NIBS) and collects data at a fixed scattering angle of 173° that significantly reduces multiple scattering and also scattering from dust and similar bigger particles. A quartz cell with a 10 mm path length was used to measure 300 μL of the sample. EmrE samples were prepared in DDM solution buffer at 500:1 molar ratios of QCC:EmrE in the presence of EB, MV, CTP and TPP. The temperature was maintained at 25 °C during all experiments.

During DLS experiments, using the intensity autocorrelation function, the relaxation rate, Γ, can be extracted and used to determine the translational diffusion coefficient, D, of the particles (EmrE proteins in this study) using the relation $D=\Gamma/Q^2$. Q is the

magnitude of the scattering vector and given by

$$Q = (4\pi n/\lambda)\sin\theta \quad (1)$$

where n refers to the refractive index of the solution, λ is the wavelength of the scattered light, and 2θ is the scattering angle. The viscosity of the water was taken as 8.9×10^{-4} Pa s and its refractive index as 1.33 at the measurement temperature of 25 °C. The diffusion coefficients of the dispersed particles can be determined from the intensity of the autocorrelation function measured by DLS experiments. Hydrodynamic radius, R_h, can then be calculated from the diffusion coefficients, D, by using the Stokes–Einstein relation

$$R_h = (k_B T)/6\pi\eta D \quad (2)$$

where $k_B T$ is the thermal energy and η is the viscosity of the dispersion medium. For the dispersions with the presence of multiple species, a regularized fit to the DLS data was applied since it gives details on the size distribution of the dispersed particles. All the values, presented in this study, were obtained using the software (V 7.02) provided by the Malvern with the instrument.

2.7. Fluorescence spectroscopy

Fluorescence spectroscopy data were collected using a Fluorolog-spectrofluorimeter from the proteins, solubilized in buffered DDM, in the presence and absence of QCCs. Sample spectra were collected in a 10 mm quartz cuvette at excitation wavelengths between 275 and 305 nm to study the dynamics of the proteins. Sets of spectra for both UT- and T-EmrE in the presence of QCCs were also collected at an excitation wavelength of 295 nm to specifically excite tryptophans. Emission spectra were measured from 285 to 400 nm using double monochromators for both excitation and emission to reduce scattering artifacts. A 5 nm band pass was used for both excitation and emission. The wavelength collection intervals were set at 0.15 nm and integration time of 0.1 s. Each collected spectrum was an average of 3 scans for each sample. All the fluorescence spectra were collected for three biological replicates ($N=3$) and the data were averaged. Error bars were calculated as standard deviation over three biological replicates. Experiments were conducted for the concentration of 0.5 μM of both UT- and T-EmrE proteins. The samples were titrated using the stock solutions of QCC in DDM buffer for QCC:EmrE molar ratios of 0.01–500. Time between each data set or the QCC titration increment was 10 min. The samples were continuously mixed using a magnetic stir bar at room temperature during the experiments. Separate sets of experiments were also performed to ensure that all the fluorescence intensity reductions were due to quenching. For this, DDM buffer was added to its respective protein sample without QCC to the same final volume of all QCC additions during the titration experiment and no changes in emission maxima were observed. All the collected fluorescence spectra were corrected for their respective background Raman spectra. Data from the blank solutions (without proteins) at each QCC concentration and excitation wavelength were collected in the DDM buffer, which were than subtracted from their relevant EmrE:QCC titration runs and excitation wavelengths.

Fluorescence emission spectra from UT- and T-EmrE, gave higher emission for the excitation wavelengths below 295 nm because of the contribution from Tyrosines whereas the emission intensity decreased beyond the excitation wavelength of 295 nm. All the spectra, between 275 and 305 nm excitation wavelength, were normalized and the positions of the peaks were compared for both UT- and T-EmrE to calculate REES effects. Spectra, collected at the excitation wavelength of 295 nm were used to obtain ligand-binding curves for QCCs with increasing molar ratios of QCC:EmrE. Intensity loss in the emission spectra was observed as the ligand/QCC binding to Trp. This data against the increasing concentration of the respective QCC was fitted using Eq. (3) to obtain the ligand-binding curves:

$$\text{Specific binding} = B_{max}[\text{ligand}]/(K_d + [\text{ligand}]) \quad (3)$$

where the fluorescence intensity change is a measure of specific binding, K_d is an apparent dissociation constant which is the concentration of ligand to reach half maximal binding, B_{max} is the maximum specific one-site binding or maximum number of binding sites, [ligand] is the ligand/QCC concentration.

The percentage loss in the peak intensity (λ_{max} average between 333 and 335 nm), caused by the Trp fluorescence quenching, was plotted against the respective QCC concentration. Data were then fitted using Eq. (3) to obtain K_d and B_{max} values as discussed below. Differences in K_d between UT- and T-EmrE were compared to understand the equivalence of the respective purification protocols and the presence of the tag. During the calculations, inner filter effects were essentially negligible.

3. Results

3.1. Differences between UT-EmrE and T-EmrE resistance to QCCs

In vivo QCC Kill curve resistance assays of plasmid transformed UT-EmrE and T-EmrE in *E. coli* were performed to functionally compare how well each protein version mediates EB and MV resistance when expressed under identical conditions. The resistance profiles of *E. coli* transformed with UT-EmrE or T-EmrE are shown in Fig. 2. After 26 h of growth, the $OD_{550\ nm}$ values

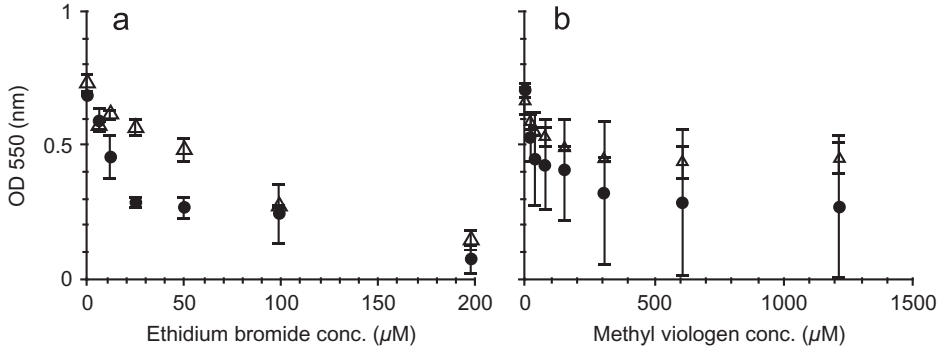

Fig. 2. QCC resistance profiles of *E. coli* overexpressing UT-EmrE and T-EmrE. $OD_{550\ nm}$ representing the growth of *E. coli* cells containing UT-EmrE (hollow triangles) or T-EmrE (solid circles) in the presence of increasing concentrations of (a) EB and (b) MV in LB growth media. $OD_{550\ nm}$ values were taken after 26 h of growth at 37 °C at different concentrations of the QCCs. All QCC resistance assays were performed in triplicate ($N=3$) and the error bars show the standard deviation.

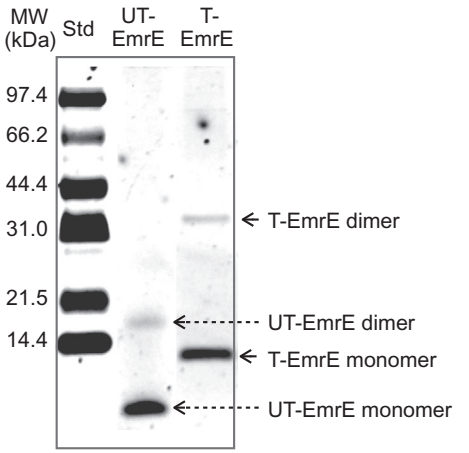

Fig. 3. SDS-Tricine 12% PAGE analysis of 0.08% w/v DDM purified UT-EmrE and T-EmrE, 1.4 μg of each protein was loaded in the respective lane. Low molecular weight (LMW) Bio-Rad protein standards were used to estimate protein weights and relative band intensity. The presence of monomeric and dimeric states are indicated for each version of EmrE by labeled arrows.

demonstrated that UT-EmrE provides more resistance to EB as compared to T-EmrE. The profile with MV was also displayed a difference but with more variability between trials.

3.2. Purification methods lead to differences in multimeric state distributions

In this study, two forms of EmrE protein UT-EmrE and T-EmrE were purified in buffered 0.08% DDM, as it is the most frequently used detergent to reconstitute the protein and maintains a—helical structure of membrane proteins [22]. Following affinity purification, the yield of T-EmrE in 0.08% DDM buffer was determined to be 0.1 mg/L. Organically extracted UT-EmrE preparations gave 0.07 mg/L of the proteins. Before solubilization in DDM buffer, the yield of organically purified dried UT-EmrE was 0.24 mg/L, indicating that only ~1/3 of the proteins could be solubilized in DDM buffer. This indicated that both tagged and untagged proteins were solubilised in DDM to similar extents.

UT-EmrE and T-EmrE, both purified in DDM are shown in Fig. 3 in their respective lanes on SDS-Tricine 12% PAGE gel to identify protein purity and multimeric forms. The molecular weight of UT-EmrE and T-EmrE monomers was estimated to be 12.2 kDa and 14.4 kDa respectively. Both purification methods provided highly pure protein (95% based on gel detection). PAGE analysis revealed that both proteins predominated as monomeric bands (88% UT-EmrE and 89% T-EmrE total protein band intensity), and as less abundant dimeric state (12% UT-EmrE and 11% T-EmrE).

The results of dynamic Light Scattering (DLS) analysis of both protein versions with and without QCC:EmrE molar ratio of 500:1 are shown in Fig. 4. The scattering intensity distribution from UT-EmrE showed peaks at R_h between 2–3, 60–70, and 200–250 nm. The R_h of T-EmrE occurred between 2–3 and 100–150 nm. Multiple intensity peaks suggest the presence of multiple species in the dispersed samples. There is a clear difference in the amount and population distributions in the plots in Fig. 4. Even the distribution of the monomer peak is quite broad suggesting manifold of folding states within the DDM micelles.

3.3. Fluorescence spectrophotometry reveals that UT-EmrE has a less constrained structure compared to T-EmrE

Fluorescence spectrophotometry was used to evaluate the conformational integrity of the different constructs. Considerable differences were observed in the fluorescence emission spectra between UT-EmrE and T-EmrE. Fluorescence spectra, collected at different excitation wavelengths between 275 and 305 nm to select for aromatic residue emission in UT-EmrE and T-EmrE samples as shown in Fig. 5. The spectral shape and maximum reflected the environment of the aromatic residue fluorophores (due to solvent polarity and dynamics) as well as the degree of energy transfer between fluorophores of Tyr to Trp.

Fluorescence emission spectra from UT-EmrE and T-EmrE, in response to the different excitation wavelengths can be analyzed to see the Red-Edge Excitation Shift (REES). This is an intrinsic property of protein fluorophores and is due to slow relaxation and re-orientation of the solvent in a viscous environment [29]. To compare the polarity and energy transfer occurring between the aromatic residue environments of UT-EmrE and T-EmrE using REES analysis, the position of the peak maximum (λ_{max}) in the emission spectrum of either protein in Fig. 5 was plotted against the excited wavelengths as shown in Fig. 6. UT-EmrE (Fig. 6a) demonstrated a peak at λ_{max}~333 nm, which was consistent for all excitation wavelengths, indicating enhanced hydrophobicity in the environment surrounding its aromatic residues. Another peak (shoulder) at λ_{max}~348 nm can also be seen in UT-EmrE that becomes prominent for the excitation wavelength at 300 nm indicating some Trp exposure to aqueous environments. This shoulder is likely a result of uncoupled energy transfer between tryptophans of different environments.

In contrast, the REES plot of T-EmrE demonstrated a single peak at all excitation wavelengths (Fig. 6b). T-EmrE emission spectra were comparable in shape for λ_{max} between 332 and 338 nm for the excitation wavelengths between 275 and 295 nm. At the excitation wavelength of 305 nm, the T-EmrE emission peak completely shifted at 388 nm. This could be due to the local solvation environment (the local residues around each of the tryptophans) having restricted dynamics. As a comparison, N-acetyl-tryptophan amide in the same buffer shows a uniform single peak (355 nm) spectrum at all excitation wavelengths (data not shown). These spectra demonstrated that neither protein has any degree of unfolding that completely exposed their tryptophans to the aqueous environment. However, the environment of fluorophore solvation and dynamics were quite different between the each version of the protein.

3.4. QCC-ligand binding reveal different UT-EmrE and T-EmrE affinities for specific ligands

The intrinsic Trp fluorescence quenching upon ligand binding was exploited to produce ligand binding curves. UT-EmrE and T-EmrE proteins were examined in the presence of four different QCC ligands: EB, MV, CTP and TPP. Ligand addition to either protein leads to a decrease in the fluorescence maximum emission peak intensity of Trp, which was influenced by its environment polarity/hydrophobicity. Changes in maximum emission peak intensity can be plotted against the concentration of ligand (QCC) to determine binding dissociation constant (K_d) for the ligand. QCC fluorescence quenching spectra, provided in Fig. 7, were curve fit to estimate the values of K_d and B_{max} for each QCC to each protein version. The results from this analysis indicated that all QCCs tested quenched Trp in UT-EmrE and T-EmrE samples and bound to both proteins (Table 2). MV and CTP had lower K_d values for UT-EmrE as compared to the T-EmrE, whereas for EB and TPP, K_d values were lower for T-EmrE. This shows that EB and TPP bound more tightly to T-EmrE as compared to UT-EmrE, whereas MV and CTP bind more tightly to the UT-EmrE.

Since ligand binding affinity depended not only on the specific arrangement of Trp at the binding site, but also depended on its access to the binding site (B_{max}). B_{max} at 100% fluorescence intensity loss for each protein indicated the binding of ligand to

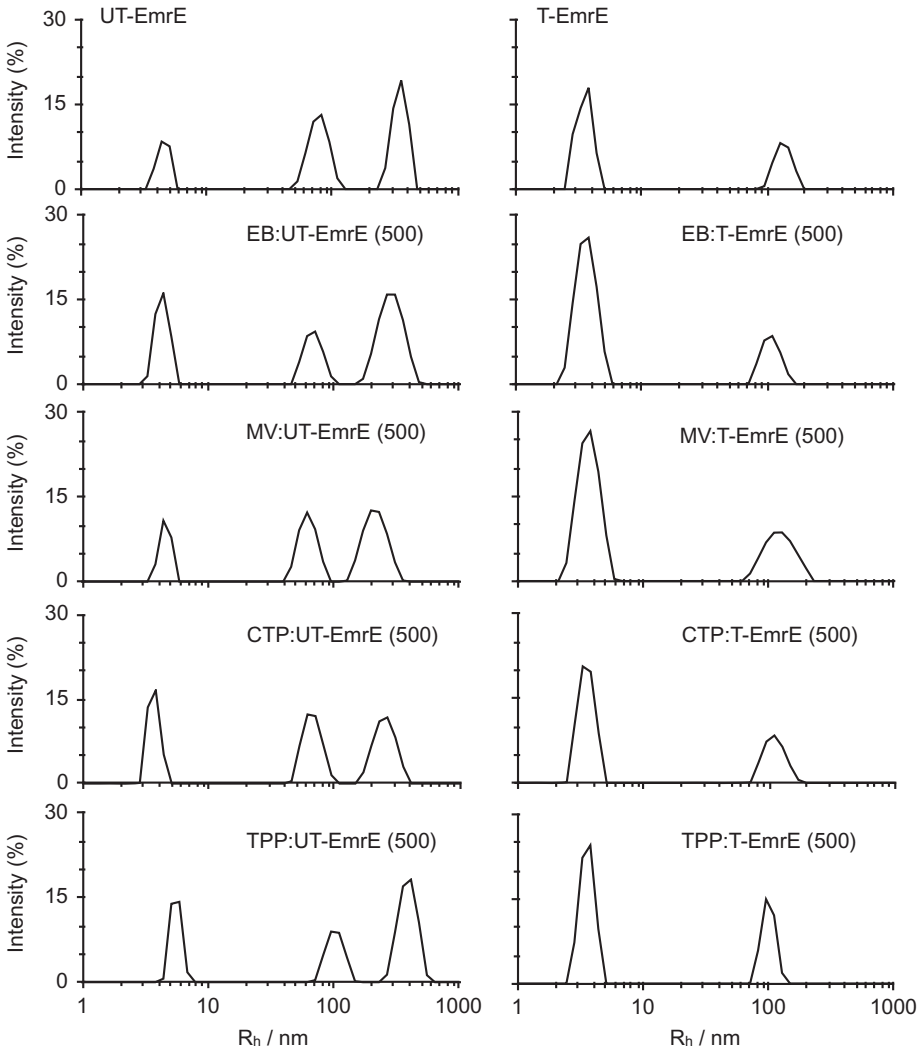

Fig. 4. DLS intensity distribution of UT-EmrE and T-EmrE in the presence of QCC. Addition of QCCs did not induce any extra peak. Molar ratios for all QCC:(T, UT) EmrE were 500:1.

each protein in DDM. Both UT-EmrE and T-EmrE had similar B_{max} values for MV and EB (Table 2), indicating that almost all the binding sites were occupied, as their fluorescence intensity loss was 100% (Fig. 7). 50% of UT-EmrE binding sites remained unoccupied for TPP (B_{max}∼50.8) in comparison to 84% of unoccupied T-EmrE binding sites with TPP (B_{max}∼16.5). In the case of CTP, some of the binding sites also remained unoccupied for T-EmrE (B_{max}∼95.4) whereas for UT-EmrE they were fully occupied (B_{max}∼103.0).

4. Discussion

The purpose of this study was to compare structural and functional characteristics of His_6-*myc* epitope tagged EmrE (T-EmrE) to untagged EmrE (UT-EmrE). Previous studies demonstrated that the His_6 tag commonly added to EmrE required a *myc* epitope sequence extension before the his_6 tag at the C-terminus of the protein [5]. In this study, both versions of EmrE were expressed in *E. coli* using the identical vector and cloning site orientations and solubilized in the same detergent and buffer. Both UT-EmrE [9,21] and T-EmrE [22] were purified using two previously published procedures involving Ni-affinity chromatography [22] to purify T-EmrE and an organic solvent extraction reverse-phase size exclusion chromatography method [7] to isolate UT-EmrE. Both versions of EmrE were purified in buffered 0.08% w/v DDM detergent which were 10 fold higher than the CMC. Both purification methods were used in this study to compare how each method influenced the structure and folding of EmrE using the same experimental evaluations. It also provided an opportunity to determine the influence the tag had on EmrE function in *E. coli* using *in vivo* drug resistance kill curve titrations (Fig. 2). It is important to note here that attempts to isolate T-EmrE using the organic extraction method were unsuccessful and failed to isolate significant amounts of T-EmrE (less than 5%) by comparison of UT-EmrE (unpublished results). The lack of T-EmrE purification by organic extraction was due to the increased hydrophilicity (11% increase compared to UT-EmrE) caused by the addition of the tag. The addition of a protease cleavable tag to EmrE is also in progress, but preliminary results indicated these preparations had low cleavage efficiency in DDM (unpublished results). Since the majority of studies of EmrE have maintained the presence of the tag (as reviewed by Bay et al. [2]), it was important for this analysis to examine the commonly used tagged version of this protein.

This study represent the first study to directly compare tagged and untagged versions of EmrE purified using their specific isolation methods and then evaluate differences in structural arrangements by SDS-Tricine PAGE, dynamic light scattering, and fluorescence spectrophotometry. These analyses also permitted

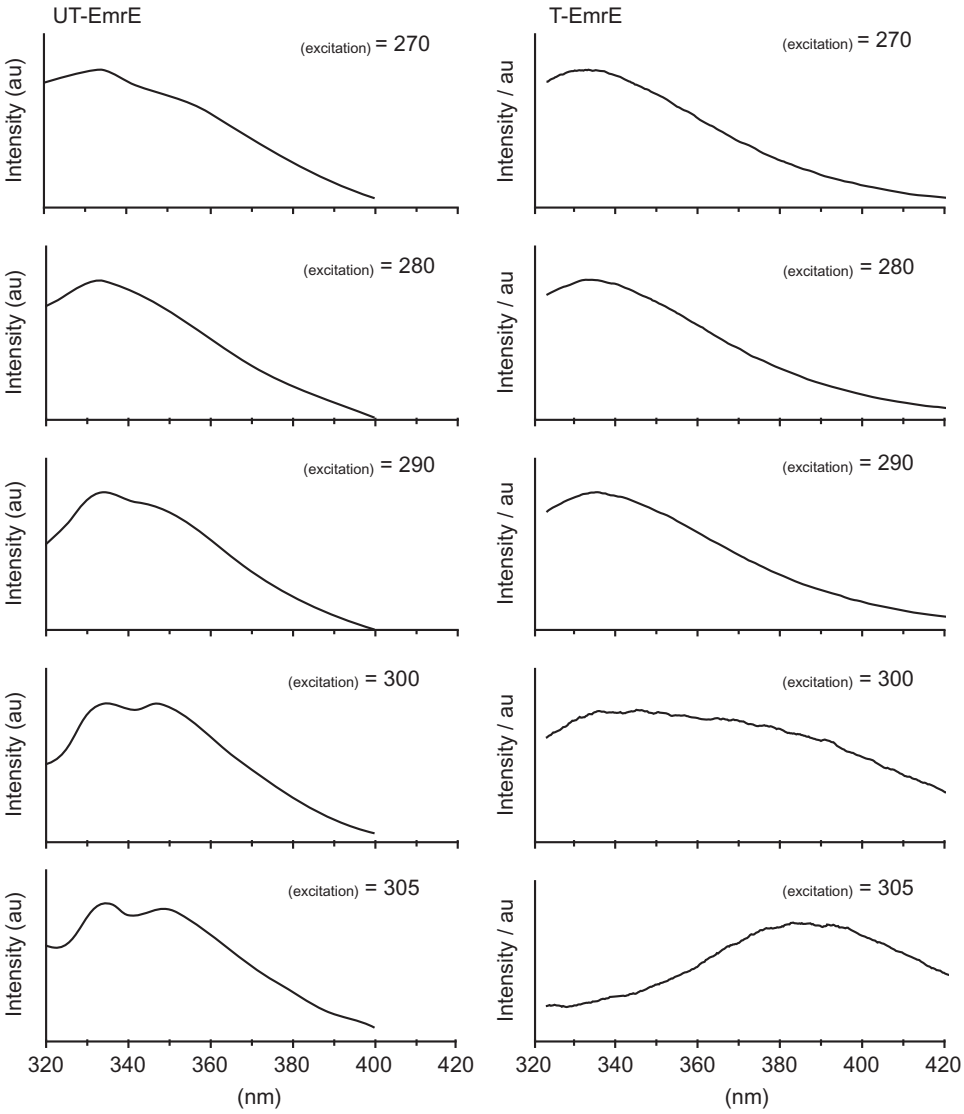

Fig. 5. Fluorescence emission spectra collected for UT-EmrE and T-EmrE at excitation wavelengths between 275 and 305 nm. All emission spectra shown in the right-hand column correspond to T-EmrE and UT-EmrE sample spectra are shown in the left-hand column. The excitation wavelength used to excite each sample is provided at top right hand corner of each emission spectrum shown. Emission spectra from either protein sample was collected at 0.5 μM protein in 0.08% DDM buffer (averaged over three runs).

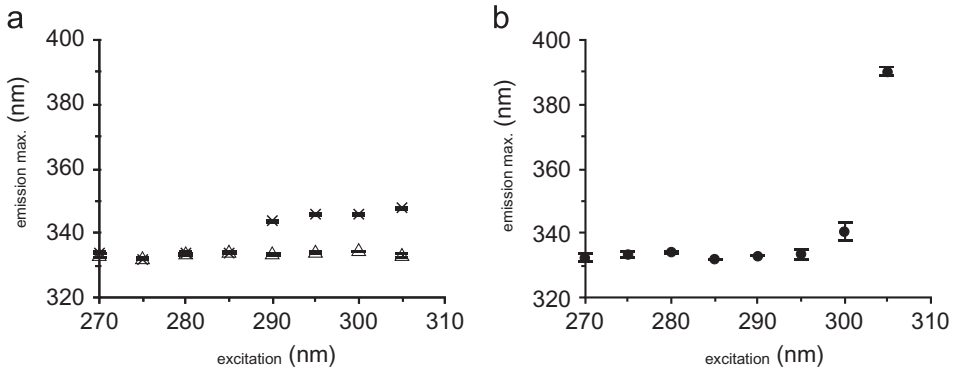

Fig. 6. Red-Edge Excitation Shift (REES) analysis of UT-EmrE and T-EmrE. Both plots showed the excitation wavelength versus emission maximum measured for each protein version: (a) REES plot of UT-EmrE produced 2 peaks, hollow triangles represented peak 1 and cross symbols indicated peak 2. (b) The single REES plot T-EmrE peak is shown that shifts towards higher emission wavelengths above 300 nm excitation wavelength.

the determination of differences in ligand binding by each protein version. The unique differences determined for each purified EmrE version in 0.08% w/v DDM in this study reflect differences in the EmrE functionality, structure, folding, and dynamics associated to the addition of the tag and/or by purification method. The presence of the tag did not alter multimerization but did appear to alter

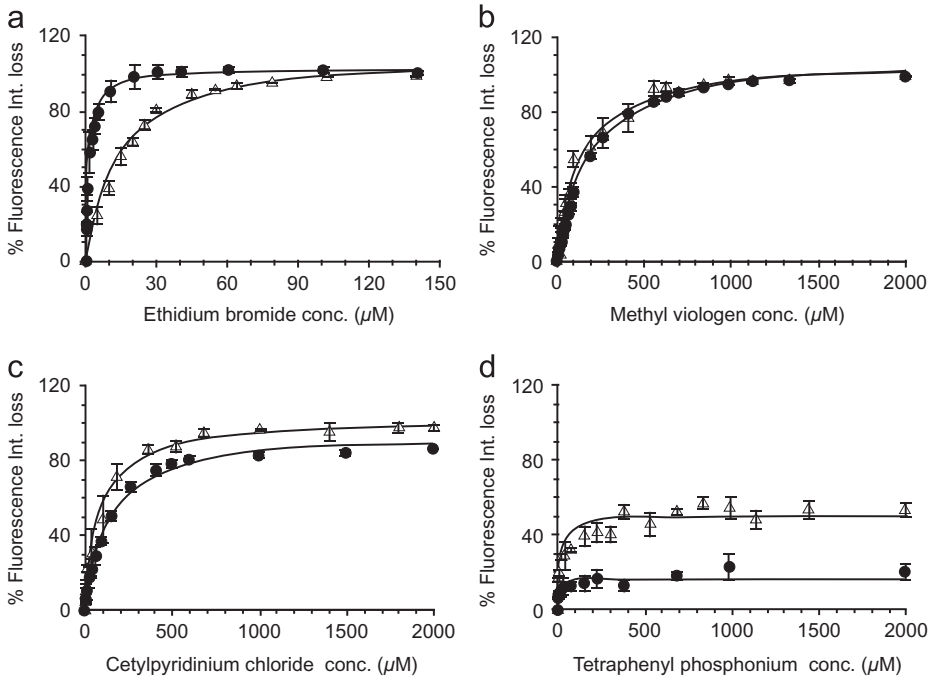

Fig. 7. QCC Trp fluorescence quenching spectra of UT-EmrE and T-EmrE. In each panel, the QCCs, EB (a), MV (b), CTP (c) and TPP (d) were examined. In all panels, symbols represent the average spectral intensity values of UT-EmrE shown as hollow triangles and T-EmrE as solid circles. Continuous lines are the fit curves to the data using Eq. (3) in the methods section. K_d values and B_{max} values representing the projected end-point of the ligand titration were obtained from the fit curves and provided in Table 2. All QCC titration samples were measured in triplicate ($N=3$) and all error bars show standard deviations at each measurement.

Table 2
A summary of the QCC binding affinities of UT-EmrE and T-EmrE determined from Trp fluorescence quenching assays.

QCC	T-EmrE			UT-EmrE		
	K_d (μM)	B_{max}	R^2	K_d (μM)	B_{max}	R^2
EB	1.3 ± 0.3	102.9 ± 1.1	0.937	13.4 ± 2.5	111.3 ± 3.9	0.973
MV	178.5 ± 19.9	110.7 ± 2.3	0.996	133.7 ± 23.7	107.8 ± 2.9	0.972
CTP	136.5 ± 20.4	95.4 ± 3.8	0.994	84.3 ± 25.8	103.0 ± 5.9	0.985
TPP	4.7 ± 3.7	16.5 ± 2.0	0.854	16.4 ± 11.3	50.8 ± 4.4	0.847

ligand interactions suggesting that the tag may enhance or reduce interactions with particular ligands as shown in fluorescence analysis. This study also compared *in vivo E. coli* QCC resistance assays for UT-EmrE and T-EmrE and identified a slight advantage by UT-EmrE to mediate resistance to EB (Fig. 2). The presence of the tag may have influenced EB transport through several means: occluding the binding site, preventing proper multimerization, or influencing the topological state. Although MV resistance appears to also demonstrate enhanced resistance by UT-EmrE, the error in UT-EmrE sample measurements may be linked to the properties of MV itself as it is known to induce oxidative cell damage and absorb within the 600 nm region [30,31]. These factors likely contributed to the high variability observed in these experiments.

Evaluation of UT-EmrE and T-EmrE multimeric forms using SDS-Tricine PAGE determined that both purification techniques resulted in gel-quality pure (95%) proteins. Since SDS is not denaturing to EmrE and has demonstrated the ability to solubilize EmrE [9] and maintain DDM-EmrE induced folding [28], PAGE analysis permitted examination of UT-EmrE and T-EmrE multimeric forms [9]. Both EmrE versions predominated in as monomers and to lesser extent as dimers indicating that the presence of tag did not significantly alter the multimer capacity of T-EmrE, in agreement with previous studies [14,23,28]. High amounts of T-EmrE monomer have been reported in previous experiments that specifically examined T-EmrE multimerization [28]. There is no clear evidence to date, that confirms the monomer state of T-EmrE or UT-EmrE are improperly folded as compared to dimers. Studies of monomeric UT-EmrE have indicated that the monomer was capable of binding QCC [8,10,16,29]. The high proportion of EmrE monomer isolation by both T-EmrE and UT-EmrE from the membranes may indicate that the dimer form is stabilized by the presence of ligand. Our previous work examining the ligand induced multimerization of UT-EmrE supports this mechanism involving monomer to dimer/higher multimer formation in the presence of ligand (as described in the review by Bay et al. [2]).

Further evaluation of UT-EmrE and T-EmrE multimeric forms by DLS demonstrated that each protein version had three (UT-EmrE) or two (T-EmrE) size states (Fig. 4). R_h values were used to estimate the molecular weight of the protein, where R_h is the radius of the sphere. For other shapes, such as plates or cylindrical particles, the R_h strongly depends on the long axes [32,33]. In the case for non-globular proteins such as EmrE, the shape of the protein includes the DDM molecules around them. Because of this, the molecular mass of UT-EmrE and T-EmrE could not be easily estimated and the values reflected should be much higher than the actual molecular mass of the proteins and its associated multimeric form. Although, the scattering intensity distribution, provided information on the presence and range of sizes in the sample, the scattering caused by bigger to smaller particles creates huge differences and the scattering intensity distribution must be weighted to account for the bigger particles in the samples containing multiple species. Therefore, large peaks at higher R_h were not an indication of a larger amount of large protein/detergent particles. Taking this into consideration, the presence of two peaks for T-EmrE suggested that it consist of primarily two different multimeric states whereas the third peak in UT-EmrE may represent a higher multimeric form. Large aggregations of EmrE have been observed previously in lipid domain experiments where lipid type and lateral membrane pressure may play a role [34,35].

It should be noted that the purification methods used to isolate UT-EmrE and T-EmrE likely affect the protein dynamics after DDM solubilization. These solubilization condition differences may change the associated counter ions, the amount of detergent molecules bound by each protein, and potentially localized unfolded regions that influence the oligomerization state [7,17,36]. Despite all these potential influences, both UT-EmrE and T-EmrE possessed similar monomeric and dimeric formation capacity (Figs. 2 and 3), but UT-EmrE had greater conformational variation (Fig. 4). Because the structure and folding of each protein may differ during the purification and solubilization procedure, tryptophans and tyrosines could be exposed to more viscous conditions than in free solution, thereby restricting the re-orientation of solvent and alter REES. This property was used to probe any differences between the relative dynamics of the fluorophore environment within UT-EmrE and T-EmrE. In this study, both UT-EmrE and T-EmrE possessed the same number of Trp residues and T-EmrE possessed an additional Tyr within the *myc*-His_6 tag. Previous studies have examined the tagged version of EmrE, and identified that only Tyr40 and Trp63 were associated with the ligand binding site Glu14 [37]. The emission spectrum of tagged EmrE below 295 nm excitation wavelength was also shown to be heavily influenced by Trp63 [17]. The red-shifted emission spectrum of T-EmrE reflected an environment that restricted solvent re-orientation (Figs. 5 and 6). A red-shifted emission can be the result of interactions of Trp and Tyr fluorophores with nearby protein residues in the binding cavity of EmrE. This suggests that the tryptophans are in a viscous or tight folded environment and could be indicative of a well-folded protein that restricts conformational freedom. In contrast to T-EmrE, a blue-shifted emission peak at 333 nm was also observed in UT-EmrE and this emission maxima did not disappear, or show reverse relaxation (Fig. 6). This type of relaxation occurs when the emission lifetime of the fluorophore is comparable to the lifetime of solvent relaxation [38]. In the case of UT-EmrE, the peak at 333 nm may have been due to reverse-relaxation of the solvent caused by the sample's longer excitation wavelengths. Additionally, this may suggest that the tryptophans in UT-EmrE were in an environment that was less constrained than the tryptophans in T-EmrE.

The conformational differences between UT-EmrE and T-EmrE observed after SDS-Trcine PAGE, DLS and fluorescence REES analyses, likely affected their affinity for particular ligands (Fig. 7). Each ligand was selected based on its chemical structure, shape and charge. MV was the only divalent cation in this study, all others are monovalent. MV and EB were planar in comparison to CTP, that had a long acyl chain and acts as a surfactant. Similar to CTP, TPP is also a surfactant but has a spherical conformation. The binding site of EmrE is located within the transmembrane region which incorporates a single highly conserved anionic residue, Glu14 [5] that facilitates both H^+ and QCC antiport [39]. In addition to Glu14, specific Trp residues like Trp63 in EmrE may participate in a cation–pi interaction with protons (as described by Dougherty [40]) based on Trp mutation studies of T-EmrE [17]. The structure of the QCC had different effects on the K_d and B_{max} values of T-EmrE compared to UT-EmrE. The interaction of T-EmrE differed from UT-EmrE for CTP and TPP. CTP may prefer to form micelles in the presence of T-EmrE, and the saturation of CTP occurred at slightly lower B_{max} values as compared to UT-EmrE. In the case of TPP, its charged cation was at the center of the molecule and was poorly accessible for both UT- and T-EmrE resulting in lower B_{max} values for both proteins. TPP appeared to have more difficulty in binding to T-EmrE but when it was bound TPP had a higher apparent affinity with lower site occupancy. The tighter affinity by T-EmrE for EB compared to UT-EmrE may also explain why *in vivo* EB resistance assays in *E. coli* showed improved EB resistance by UT-EmrE expressing strains.

5. Conclusions

Structural and functional comparison of T-EmrE and UT-EmrE revealed differences in QCC resistance profiles, structural conformation, and ligand binding between the different forms. It also highlights differences in EmrE folding that may be attributed not only to the presence of a tag but also due to differences in purification methodologies. Although both forms of the protein have similar multimeric forms, bind the same ligands, and confer resistance to the same QCCs, the differences help to explain the frustrations over the years between different research group's data. Thus this work helps interpret results from previous studies that have examined tagged and untagged forms of EmrE and other groups studying integral membrane protein transporters or other integral membrane proteins tagged in a similar fashion.

Acknowledgments

We would like to acknowledge funding for this work from Alberta Innovates – Health Solutions (AIHS) postdoctoral fellowship to S.J.S. Qazi's and research support from Natural Sciences and Engineering Research Council of Canada (NSERC) – Discovery Grant RGPIN/216887 to R.J.T.

Appendix A. Transparency document

Transparency document associated with this article can be found in the online version at http://dx.doi.org/10.1016/j.bbrep.2015.03.007

References

[1] I.T. Paulsen, R.A. Skurray, R. Tam, M.H. Saier, R.J. Turner, J.H. Weiner, et al., The SMR family: a novel family of multidrug efflux proteins involved with the efflux of lipophilic drugs, Mol. Microbiol. 19 (1996) 1167–1175. http://dx.doi.org/10.1111/j.1365-2958.1996.tb02462.x.

[2] D.C. Bay, K.L. Rommens, R.J. Turner, Small multidrug resistance proteins: a multidrug transporter family that continues to grow, Biochim. Biophys. Acta (BBA) – Biomembr. 1778 (2008) 1814–1838. http://dx.doi.org/10.1016/j.bbamem.2007.08.015.

[3] H. Yerushalmi, M. Lebendiker, S. Schuldiner, EmrE, an *Escherichia coli* 12-kDa multidrug transporter, exchanges toxic cations and H+ and is soluble in organic solvents, J. Biol. Chem. 270 (1995) 6856–6863.

[4] H. Yerushalmi, M. Lebendiker, S. Schuldiner, Negative dominance studies demonstrate the oligomeric structure of EmrE, a multidrug antiporter from *Escherichia coli*, J. Biol. Chem. 271 (1996) 31044–31048. http://dx.doi.org/10.1074/jbc.271.49.31044.

[5] T.R. Muth, S. Schuldiner, A membrane-embedded glutamate is required for ligand binding to the multidrug transporter EmrE, EMBO J. 19 (2000) 234–240. http://dx.doi.org/10.1093/emboj/19.2.234.

[6] I. Ubarretxena-Belandia, J.M. Baldwin, S. Schuldiner, C.G. Tate, Three-dimensional structure of the bacterial multidrug transporter EmrE shows it is an asymmetric homodimer, EMBO J. 22 (2003) 6175–6181.

[7] T.L. Winstone, M. Jidenko, M.L. Maire, C. Ebel, K.A. Duncalf, R.J. Turner, Organic solvent extracted EmrE solubilized in dodecyl maltoside is monomeric and binds drug ligand, Biochem. Biophys. Res. Commun. 327 (2005) 437–445. http://dx.doi.org/10.1016/j.bbrc.2004.11.164.

[8] Y.-J. Chen, O. Pornillos, S. Lieu, C. Ma, A.P. Chen, G. Chang, X-ray structure of EmrE supports dual topology model, Proc. Natl. Acad. Sci. USA 104 (2007) 18999–19004. http://dx.doi.org/10.1073/pnas.0709387104.

[9] D.C. Bay, R.A. Budiman, M.-P. Nieh, R.J. Turner, Multimeric forms of the small multidrug resistance protein EmrE in anionic detergent, BBA – Biomembranes 1798 (2010) 526–535. http://dx.doi.org/10.1016/j.bbamem.2009.12.017.

[10] M. Schwaiger, M. Lebendiker, H. Yerushalmi, M. Coles, A. Groger, C. Schwarz, et al., NMR investigation of the multidrug transporter EmrE, an integral membrane protein, Eur. J. Biochem. 254 (1998) 610–619. http://dx.doi.org/10.1046/j.1432-1327.1998.2540610.x.

[11] J. Porath, J. Carlsson, I. Olsson, G. Belfrage, Metal chelate affinity chromatography, a new approach to protein fractionation, Nature 258 (1975) 598–599.

[12] K. Terpe, Overview of tag protein fusions: from molecular and biochemical fundamentals to commercial systems, Appl. Microbiol. Biotechnol. 60 (2003) 523–533. http://dx.doi.org/10.1007/s00253-002-1158-6.

[13] S. Schuldiner, EmrE, a model for studying evolution and mechanism of ion-coupled transporters, Biochim. Biophys. Acta 2009 (1794) 748–762. http://dx.doi.org/10.1016/j.bbapap.2008.12.018.
[14] C.G. Tate, I. Ubarretxena-Belandia, J.M. Baldwin, Conformational changes in the multidrug transporter EmrE associated with substrate binding, J. Mol. Biol. 332 (2003) 229–242. http://dx.doi.org/10.1016/S0022-2836(03)00895-7.
[15] C.G. Tate, Comparison of three structures of the multidrug transporter EmrE, Curr. Opin. Struct. Biol. 16 (2006) 457–464. http://dx.doi.org/10.1016/j.sbi.2006.06.005.
[16] I. Lehner, D. Basting, B. Meyer, W. Haase, T. Manolikas, C. Kaiser, et al., The key residue for substrate transport (Glu14) in the EmrE dimer is asymmetric, J. Biol. Chem. 283 (2008) 3281–3288. http://dx.doi.org/10.1074/jbc.M707899200.
[17] Y. Elbaz, N. Tayer, E. Steinfels, S. Steiner-Mordoch, S. Schuldiner, Substrate-induced tryptophan fluorescence changes in EmrE, the smallest ion-coupled multidrug transporter, Biochemistry. 44 (2005) 7369–7377. http://dx.doi.org/10.1021/bi050356t.
[18] D. Rotem, N. Sal-man, S. Schuldiner, In vitro monomer swapping in EmrE, a multidrug transporter from *Escherichia coli*, reveals that the oligomer is the functional unit, J. Biol. Chem. 276 (2001) 48243–48249. http://dx.doi.org/10.1074/jbc.M108229200.
[19] P.J.G. Butler, I. Ubarretxena-Belandia, T. Warne, C.G. Tate, The *Escherichia coli* multidrug transporter EmrE is a dimer in the detergent-solubilised state, J. Mol. Biol. 340 (2004) 797–808. http://dx.doi.org/10.1016/j.jmb.2004.05.014.
[20] C.W. Sikora, R.J. Turner, Investigation of ligand binding to the multidrug resistance protein EmrE by isothermal titration calorimetry, Biophys. J. 88 (2005) 475–482. http://dx.doi.org/10.1529/biophysj.104.049247.
[21] T.L. Winstone, K.A. Duncalf, R.J. Turner, Optimization of expression and the purification by organic extraction of the integral membrane protein EmrE, Protein Expr. Purif. 26 (2002) 111–121.
[22] D. Miller, K. Charalambous, D. Rotem, S. Schuldiner, P. Curnow, P.J. Booth, In vitro unfolding and refolding of the small multidrug transporter EmrE, J. Mol. Biol. 393 (2009) 815–832. http://dx.doi.org/10.1016/j.jmb.2009.08.039.
[23] D.C. Bay, R.J. Turner, Small multidrug resistance protein EmrE reduces host pH and osmotic tolerance to metabolic quaternary cation osmoprotectants, J. Bacteriol. 194 (2012) 5941–5948. http://dx.doi.org/10.1128/JB.00666-12.
[24] M.S. Beketskaia, D.C. Bay, R.J. Turner, Outer membrane protein OmpW participates with small multidrug resistance protein member EmrE in quaternary cationic compound efflux, J. Bacteriol. 196 (2014) 1908–1914. http://dx.doi.org/10.1128/JB.01483-14.
[25] G.L. Peterson, A simplification of the protein assay method of Lowry et al. which is more generally applicable, Anal. Biochem. 83 (1977) 346–356. http://dx.doi.org/10.1016/0003-2697(77)90043-4.
[26] B. Miroux, J.E. Walker, Over-production of proteins in *Escherichia coli*: mutant hosts that allow synthesis of some membrane proteins and globular proteins at high levels, J. Mol. Biol. 260 (1996) 289–298. http://dx.doi.org/10.1006/jmbi.1996.0399.
[27] C.L. Ladner, J. Yang, R.J. Turner, R.A. Edwards, Visible fluorescent detection of proteins in polyacrylamide gels without staining, Anal. Biochem. 326 (2004) 13–20. http://dx.doi.org/10.1016/j.ab.2003.10.047.
[28] D.C. Bay, R.J. Turner, Spectroscopic analysis of small multidrug resistance protein EmrE in the presence of various quaternary cation compounds, Biochim. Biophys. Acta (BBA) – Biomembr. 1818 (2012) 1318–1331. http://dx.doi.org/10.1016/j.bbamem.2012.01.022.
[29] J.R. Lakowicz, S. Keating-Nakamoto, Red-edge excitation of fluorescence and dynamic properties of proteins and membranes, Biochemistry. 23 (1984) 3013–3021.
[30] H. Palmer, M. Ohta, M. Watanabe, T. Suzuki, Oxidative stress-induced cellular damage caused by UV and methyl viologen in Euglena gracilis and its suppression with rutin, J. Photochem. Photobiol. B Biol. 67 (2002) 116–129.
[31] C. Bagyinka, J. Osz, S. Száraz, Autocatalytic oscillations in the early phase of the photoreduced methyl viologen-initiated fast kinetic reaction of hydrogenase, J. Biol. Chem. 278 (2003) 20624–20627. http://dx.doi.org/10.1074/jbc.M300623200.
[32] S.J.S. Qazi, A.R. Rennie, J.K. Cockcroft, M. Vickers, Use of wide-angle X-ray diffraction to measure shape and size of dispersed colloidal particles, J. Colloid Interface Sci. 338 (2009) 105–110. http://dx.doi.org/10.1016/j.jcis.2009.06.006.
[33] N.A. Mazer, G.B. Benedek, M.C. Carey, Quasielastic light-scattering studies of aqueous biliary lipid systems. Mixed micelle formation in bile salt-lecithin solutions, Biochemistry 19 (1980) 601–615. http://dx.doi.org/10.1021/bi00545a001.
[34] T. Gröger, S. Nathoo, T. Ku, C.W. Sikora, R.J. Turner, E.J. Prenner, Real-time imaging of lipid domains and distinct coexisting membrane protein clusters, Chem. Phys. Lipids 165 (2012) 216–224. http://dx.doi.org/10.1016/j.chemphyslip.2011.12.012.
[35] S. Nathoo, J.K. Litzenberger, D.C. Bay, R.J. Turner, E.J. Prenner, Visualizing a multidrug resistance protein, EmrE, with major bacterial lipids using Brewster angle microscopy, Chem. Phys. Lipids 167–168 (2013) 33–42. http://dx.doi.org/10.1016/j.chemphyslip.2013.01.007.
[36] S.L. Federkeil, T.L. Winstone, G. Jickling, R.J. Turner, Examination of EmrE conformational differences in various membrane mimetic environments, Biochem. Cell Biol. 81 (2003) 61–70. http://dx.doi.org/10.1139/o03-031.
[37] M. Sharoni, S. Steiner-Mordoch, S. Schuldiner, Exploring the binding domain of EmrE, the smallest multidrug transporter, J. Biol. Chem. 280 (2005) 32849–32855. http://dx.doi.org/10.1074/jbc.M504910200.
[38] N.A. Nemkovich, V.I. Matseiko, A.N. Rubinov, V.I. Tomin, Intermolecular orientational upward relaxation in viscous solutions of organic compounds, JETP Lett. 29 (1979) 717–719.
[39] M. Soskine, Y. Adam, S. Schuldiner, Direct evidence for substrate-induced proton release in detergent-solubilized EmrE, a multidrug transporter, J. Biol. Chem. 279 (2004) 9951–9955. http://dx.doi.org/10.1074/jbc.M312853200.
[40] D.A. Dougherty, Cation–pi interactions in chemistry and biology: a new view of benzene, Phe, Tyr, and Trp, Science 271 (1996) 163–168.